

Self-similar spherical collapse with non-radial motions

Adi Nusser

Physics Department, The Technion- Israel Institute of Technology, Haifa 32000
 E-mail: adi@physics.technion.ac.il

6 March 2019

ABSTRACT

We derive the asymptotic mass profile near the collapse center of an initial spherical density perturbation, $\delta \propto M^{-\epsilon}$, of collision-less particles with non-radial motions. We show that angular momenta introduced at the initial time do not affect the mass profile. Alternatively, we consider a scheme in which a particle moves on a radial orbit until it reaches its turnaround radius, r_* . At turnaround the particle acquires an angular momentum $L = \mathcal{L}\sqrt{GM_*r_*}$ per unit mass, where M_* is the mass interior to r_* . In this scheme, the mass profile is $M \propto r^{3/(1+3\epsilon)}$ for all $\epsilon > 0$, in the region $r/r_t \ll \mathcal{L}$, where r_t is the current turnaround radius. If $\mathcal{L} \ll 1$ then the profile in the region $\mathcal{L} \ll r/r_t \ll 1$ is $M \propto r$ for $\epsilon < 2/3$. The derivation relies on a general property of non-radial orbits which is that ratio of the pericenter to apocenter is constant in a force field $k(t)r^n$ with $k(t)$ varying adiabatically.

Key words: cosmology: theory– dark matter– large scale structure of the Universe

1 INTRODUCTION

In the hierarchical scenario for structure formation, the initial density field is Gaussian with a fluctuation amplitude that decreases with scale (Peebles 1980). Non-linear gravitational evolution then causes matter to aggregate into bound virialized objects (halos) which are believed to harbor galaxies, and galaxy groups and clusters. The mass distribution in halos can be inferred from a variety of observations. These include observations of rotation curves of spiral galaxies (e.g., Persic et. al. 1996), motions of satellite galaxies (Zaritsky & White 1994), lensing distortions of background galaxy images by the potential wells of massive halos (e.g., Bartelmann & Schneider 1999), and velocity dispersion and X-ray maps of galaxy clusters (e.g., Bahcall & Fan 1998, Sarazin 1986). Nevertheless, no single observational method probes the mass profile over the entire extent of the halo. Therefore a conclusive analysis of the observations must rely on an assumed model for the halo mass profile. This is important for example in estimating the total masses of galaxy clusters. Further, halo profiles in the inner regions depend on the type of dark matter (e.g., Moore 1994). A comparison between observed and model mass profiles in the context of a given cosmological model can provide important information on the nature of dark matter.

We lack a complete theory of nonlinear gravitating systems. So a detailed study of nonlinear collapse into bound objects must rely on N-body simulations. The simulations seem to be converging on the shape of the mass profile in the halo inner regions (Navarro, Frenk & White 1997, Moore et. al. 1998, Jing 1999, Klypin et. al. 2000). As of yet no satisfac-

tory analytic explanation of the simulations results has been suggested (but see Weinberg 2000, Syer & White 1998). In a generic collapse the infalling matter is in irregular clumps undergoing dynamical friction and tidal stripping as they sink towards the center (e.g., Avila-Rees et. al. 1998, Nusser & Sheth 1999). Moreover, a collapsed object today might have gone through a merger with another object of comparable mass, a process that might have an effect on its current mass profile. Because of these factors, the focus of analytic studies has been the collapse of perturbations with special configurations. An important step forward in these studies came with the realization that the potential in the inner collapse regions varies very little over the dynamical time scale (Gunn 1977), admitting an adiabatic invariant for the motion of a particle. Using adiabatic invariance, Fillmore & Goldreich (1984, hereafter FG84, see also Bertschinger 1985) have shown that in spherical symmetry an initial density perturbation $\Delta M/M \sim M^{-\epsilon}$ develops an asymptotic mass profile $M \propto r$ near the origin for $0 < \epsilon \leq 2/3$ and $M \propto r^{3/(1+3\epsilon)}$ for $\epsilon > 2/3$. FG84 restricted their analysis to particles collapsing on purely radial orbits. Spherical collapse with non-radial particle motions has also been considered in the context of adiabatic invariance. Gurevich & Zybin (1988a,b) developed a formalism based on the theory of adiabatic capture (e.g., Lifshitz & Pitaevskii 1981), to estimate the mass profile in a spherical collapse including non-radial motions. Although their formalism can be useful to study the collapse of various initial conditions, Gurevich & Zybin applied it only to the collapse near the center of a smoothed initial density maxima. Ryden & Gunn (1987) included non-radial motions in their application of adiabatic

invariance in a numerical scheme to study the evolution of a spherical peak in a Gaussian density field (Bardeen et. al. 1986, Hoffman & Shaham 1985).

White & Zartizky (1991) described the $M \propto r$ profile for $\epsilon \leq 2/3$ in the purely radial spherical collapse in terms of the crowding of orbits as particles pass through the center. They conjectured that if particles had non-radial orbits then the crowding effect is avoided and the scaling $M \propto r^{3/(1+3\epsilon)}$ $\epsilon > 2/3$ would also be valid for $0 < \epsilon \leq 2/3$. Here we examine this conjecture in detail by generalizing the analysis of FG84. We consider two schemes for assigning angular momenta to the collapsing particles.

The outline of this paper is as follows. In section 2 we write the equations of motion and the relevant initial conditions and present two schemes for assigning angular momenta to particles. In section 3 we discuss self-similarity and adiabatic invariance in the context of non-radial motions. In section 4 we derive the asymptotic profiles for various cases. We conclude with a summary and discussion in section 5.

2 THE EQUATIONS

We consider the evolution of an isolated spherical positive density perturbation in a flat universe made of collision-less matter only (density parameter $\Omega = 1$). We describe the perturbation by a large number of equal mass particles having angular momenta in random directions such that the mean angular momentum at any point in space is zero. Spherical symmetry is then preserved and the angular momentum of each particle is conserved as the system evolves. It is often convenient here to think of a particle as a spherical shell obeying the equations of motion of a point particle moving in the gravity field of the perturbation with conserved angular momentum. We write now the equations of motion governing the evolution of a shell with a given angular momentum per unit mass, L . Denote by r be the distance from the symmetry center, and by $M(< r, t)$ the mass contained inside r at time t . The trajectory $r(t)$ of the shell as a function of time is then given by the solution to

$$\frac{d^2r}{dt^2} = -\frac{GM(< r, t)}{r^2} + \frac{L^2}{r^3}, \quad (1)$$

where the mass $M(< r, t)$ is determined from the distribution of shells at time t . Deferring the discussion of the way shells (particles) are assigned angular momenta, these equations determine the evolution of the system given a set of initial conditions specified at an early time $t_i \rightarrow 0$. We assume that the initial radial velocity of a shell at r_i is equal to the Hubble expansion velocity at t_i , that is,

$$\frac{dr_i}{dt} = \frac{2}{3t_i} r_i. \quad (2)$$

We express the initial mass distribution in terms of the relative mass excess $\delta_i \equiv \Delta M/M$ interior to an initial radius $r_i = [3M/4\pi\rho_b(t_i)]^{1/3}$ where $\rho_b(t_i) = (6\pi G t_i)^{-2}$ is the mean background density t_i . We take the scale free form

$$\delta_i = \frac{\Delta M}{M} = \left(\frac{M}{M_0}\right)^{-\epsilon}, \quad (3)$$

where $\epsilon > 0$. A perturbation with $\epsilon > 1$ can be realized by placing a point mass at the center of a void with local density contrast $\propto -M^{-\epsilon}$ (cf. Chuzhoy & Nusser 2000). In

cosmology the initial perturbations are small so we restrict the analysis to shell far enough from the center so that $\delta_i \ll 1$.

The general solution to the equations can be obtained by numerical integration where the mass distribution is continuously updated from the new positions of the shells at each time step. However the equations allow an analytic solution for the motion of a shell that has not crossed any other so that $M[< r(t)] = \text{const.}$ We will see later that for some choices of the angular momenta, this solution is applicable in the outer regions of the collapse. The solution can be written in the parametric form (e.g., Landau & Lifshitz 1976),

$$r = r_0(1 - e \cos \eta); \quad t = t_0(\eta - e \sin \eta), \quad (4)$$

where

$$e^2 = 1 + \frac{2EL^2}{G^2M^2}, \quad r_0 = \frac{L^2}{GM} \frac{1}{1-e^2}, \quad t_0 = \sqrt{\frac{r_0^3}{GM}}. \quad (5)$$

According to this solution, the shell expands until it reaches a maximum expansion radius (turnaround radius) $r_* = r_0(1+e)$, at time $t_* = \pi t_0$. The solution ceases to be valid shortly after maximum expansion when the shell crosses other shells returning from the inner regions after passing through their maximum expansion sometime ago. The expressions for r_* and t_* for purely radial motion can be recovered by taking the limit $L \rightarrow 0$ in (5). In this limit we find (cf. Peebles 1980, FG84)

$$r_* = r_0(1+e) = \frac{L^2}{GM(1-e)} \quad (6)$$

$$\approx -\frac{GM}{E} = r_i \delta_i^{-1} = \left[\frac{3M_0}{4\pi\rho_b(t_i)} \right]^{1/3} \left(\frac{M}{M_0} \right)^{1/3+\epsilon} \quad (7)$$

$$t_* = \frac{\pi}{2\sqrt{2}} \frac{GM}{|E|^{3/2}} = \frac{3\pi}{4} \left[\frac{1}{6\pi G \rho_b(t_i)} \right]^{1/2} \delta_i^{-3/2} \quad (8)$$

$$= \frac{3\pi}{4} t_i \delta_i^{-3/2} = \frac{3\pi}{4} t_i \left(\frac{M}{M_0} \right)^{3\epsilon/2}. \quad (9)$$

The solution (4) also describes the motion of a particle with non-vanishing angular momentum in an attractive force field $\propto 1/r^2$. We remark here that by taking the angular momentum to zero we do not recover the motion of a particle with zero angular momentum. In the limit $L \rightarrow 0$ the particle has zero radial velocity near the center oscillates between $r = 0$ and a maximal radius, r_* . A particle with $L = 0$ on the other hand has an infinite radial velocity at $r = 0$ and oscillates between $-r_*$ and r_* .

2.1 Two schemes for assigning angular momentum

We will consider two schemes for assigning angular momenta to particles. In the first scheme (scheme A) angular momenta are assigned at the initial time in such a way that no additional scale is introduced in the collapse. The angular momentum of each particles is conserved in the subsequent evolution of the perturbation. In the second scheme (scheme B) a particle acquires its angular momentum when it is at maximum expansion, prior to that it is assumed to have a purely radial motion. The angular momentum of a particle in scheme B is $\propto \sqrt{GM(< r_*)r_*}$ per unit mass (White & Zartizky 1991), so no additional physical scale is introduced.

In scheme A the energy per unit mass of a shell can be written in terms of the initial radius r_i and mass excess $\delta_i M_i$ inside the shell at the initial time, t_i ,

$$E = \frac{L^2}{2r_i^2} - G \frac{\delta_i M_i}{r_i}, \quad (10)$$

so to make all energy components scale similarly we choose

$$L^2 = 2\alpha G \delta_i M_i r_i = 2\alpha G \left[\frac{3}{4\pi \rho_b(t_i)} \right]^{1/3} M_0^{4/3} \delta_i^{4/3-\epsilon}, \quad (11)$$

where $1 > \alpha > 0$ insuring that the energy $E = (\alpha - 1)G\delta M_i/r_i$ is negative and the shell is bound. This choice for L does not introduce any scale in the initial conditions.

The eccentricity, e , corresponding to the motion before shell crossing is, according to (5), given by

$$e^2 = 1 + 4\alpha(\alpha - 1)\delta_i^2. \quad (12)$$

Since in cosmological perturbations the initial density contrast is small, the last relation implies that the eccentricity is very close to unity. Therefore, according to (9), the turnaround time of the shell is $t_* = t_i \delta^{-3/2} \sim r_i^{3\epsilon}$ and the turnaround radius is $r_* = r_i \delta_i^{-1} \sim r_i^{1+3\epsilon}$. This scaling means that inner shells collapse earlier than outer shells and the solution (4) is always valid outside the the radius of the shell at maximum expansion at the current time, t (hereafter, the current turnaround radius).

In scheme B, a shell moves with zero angular momentum until it reaches its turnaround radius, where it is assigned an angular momentum per units mass according to

$$L^2 = \mathcal{L}^2 G M_* r_* = \mathcal{L}^2 G \left[\frac{3}{4\pi \rho_b(t_i)} \right]^{1/3} M_0^{4/3} \delta^{4/3+\epsilon}, \quad (13)$$

where \mathcal{L} is a constant value for all shells. To insure that a shell remains bound and subsequently collapses towards the center we demand $\mathcal{L} < 1$. Note that the angular momentum assigned to a particle at the initial time in scheme A is $\propto \delta_i^2 M_* r_*$.

Shortly after reaching its turnaround radius, a shell starts its oscillations in the collective gravitational potential well generated by shells that have passed their turnaround radii at earlier times. Angular momentum introduces an effective repellent force, L^3/r^3 , preventing shells from reaching the center. We will see that in scheme A angular momentum affects the density profile only inside a radius equal to the initial radius of the shell at the current turnaround radius. For cosmological initial conditions this radius tends to zero since $t_i \rightarrow 0$. So angular momentum does not play a role in fixing the density profile of the evolved perturbation. In this case the results of FG84 for collapse of particles on purely radial orbits remain valid. In scheme B, angular momentum can prevent particles from penetrating a significant fraction, depending on \mathcal{L} , of the current turnaround radius.

3 SELF-SIMILARITY AND ADIABATIC INVARIANCE

The initial conditions are scale free, the two schemes for assigning angular momenta do not introduce any additional scale in the problem. So the only characteristic scale in the evolution of the perturbation is the scale of non-linearity

which at any time t can be taken as the current turnaround radius, $r_t(t)$. The mass scale corresponding to the current turnaround radius is $M_t = M(< r_t)$. So the mass distribution $M(r, t)$ must satisfy the self-similarity condition

$$M(r, t) = M_t \mathcal{M}(r/r_t), \quad (14)$$

where \mathcal{M} is a function of r/r_t only. Substituting $t_* = t$ in (9) we find

$$r_t = \left[\frac{3M_0}{4\pi \rho_b(t_i)} \right]^{1/3} \left(\frac{t}{t_i} \right)^{2/3+2/(9\epsilon)} \quad (15)$$

$$M_t = M_0 \left(\frac{t}{t_i} \right)^{2/(3\epsilon)}. \quad (16)$$

Assume that in some region the mass distribution can be approximated as

$$M = k(t)r^\gamma, \quad k(t) = k_0 t^{-s}, \quad (17)$$

where k_0 , s , and γ are constants*. We will determine γ in the next section by generalizing the analysis of FG84 for collapse with no angular momentum (see also Zaroubi & Hoffman 1992). However, the following useful constraint

$$s + \frac{2}{3\epsilon} - \frac{2}{3}\gamma \left(1 + \frac{2}{3\epsilon} \right) = 0, \quad (18)$$

can readily be found by substituting the asymptotic form (17) for the mass in the self-similarity condition (14) and using (16).

Throughout the rest of the paper we will assume that the potential well near the center varies adiabatically (Gunn 1977, FG84). This means that a shell near the center makes many oscillations before the potential changes significantly (Gunn 1977, FG84). In a slowly varying potential the action variables associated with the motion of a particle is invariant. The angular action variable is the angular momentum which, thanks to spherical symmetry, is conserved independent of whether or not the potential changes adiabatically. The radial action variable associated with the motion of a particle in the potential well of (17) is

$$J_r = 2\pi \int_{r_b}^{r_a} dr \left(\frac{dr}{dt} \right) \quad (19)$$

$$= \int dr \left[2 \left(E - \frac{\kappa(t)}{\gamma-1} r^{\gamma-1} \right) - \frac{L^2}{r^2} \right]^{1/2}, \quad (20)$$

where r_a and r_b are, respectively, the apocenter and pericenter of the particle's orbit. We prove now that the invariance of J_r implies that the ratio $\xi \equiv r_b/r_a$ is constant with time. This important property will simplify the determination of γ in the next section. We prove it in the following way. The energy E and κ can be expressed in terms of r_a and r_b as

$$\frac{2\kappa}{\gamma-1} = -L^2 \frac{r_a^{-2} - r_b^{-2}}{r_a^{\gamma-1} - r_b^{\gamma-1}}, \quad (21)$$

$$2E = -L^2 \frac{r_a^{-2} - r_b^{-2}}{r_a^{\gamma-1} - r_b^{\gamma-1}} r_a^{\gamma-1} + \frac{L^2}{r_a^2}. \quad (22)$$

Therefore

* For collapse described by a finite number of particles, the form (17) is meant to describe the mass averaged over a few particle oscillations within r .

$$J_r = 2\pi L \int_{\xi}^1 du \left[(\xi^{-2} - 1) \left(\frac{1 - u^{\gamma-1}}{1 - \xi^{\gamma-1}} \right) + (1 - u^{-2}) \right]^{1/2} \quad (23)$$

The angular momentum L is conserved, so the invariance of J_r means that ξ is constant. Since the only special time in the particle history is its turnaround time t_* , the invariance of ξ implies that

$$\frac{r_{a,b}}{r_*} = \left(\frac{t}{t_*} \right)^q, \quad (24)$$

near the center. The index q can be expressed in terms of γ and s by using (24) in (21). This yields

$$s = q(\gamma + 1). \quad (25)$$

4 THE ASYMPTOTIC BEHAVIOR

Assuming the asymptotic form (17) we now turn to estimating the exponents γ , s , and q . Let $P(r, r_i, t) = \int_r^{r_a} dr (dr/dt)^{-1} / \int_{r_p}^{r_a} dr (dr/dt)^{-1}$ the fraction of time a particle with initial radius r_i spends inside the radius r at the present time. The function P is well defined if the mass within r changes very little during one oscillation period of a particle inside r . The mass $M(< r, t)$ can be written in terms of P as

$$M(< r, t) = \int_0^{M_t} dM_i P(r, r_i, t), \quad (26)$$

where $M_i = 4\pi\rho_b(t_i)r_i^3/3$. By substituting (14) and (17) in this last relation we obtain

$$\left(\frac{r}{r_t} \right)^\gamma = \int_0^{M_t} \frac{dM_i}{M_t} P(r, r_i). \quad (27)$$

Following FG84 we write P in terms of $u \equiv r/r_a$. By definition, $P(u) = 0$ for $u < \xi$ and $P(u) = 1$ for $u > 1$. For $\xi \leq u \leq 1$, we write $P(u) = I(u)/I(1)$, where

$$I(u) = \int_{\xi}^u dv \left[(\xi^{-2} - 1) \left(\frac{1 - v^{\gamma-1}}{1 - \xi^{\gamma-1}} \right) + (1 - v^{-2}) \right]^{-1/2}. \quad (28)$$

Using the relations (9) and (24) we express the mass, M_i , in terms of u . So

$$\left(\frac{r}{r_t} \right)^{\gamma-p} = \frac{1}{p} \int_{r/r_t}^{\infty} du u^{-(1+p)} P(u, \xi), \quad (29)$$

where

$$p = \frac{6}{2 + 3(2 - 3q)\epsilon}. \quad (30)$$

Particles with $r_b > r$, i.e., $u = r/r_a < \xi$, have $P(u) = 0$ and do not contribute to the integral on the right hand side. The relation (29) allows us to obtain the asymptotic behavior in scheme A and B without a detailed calculation of $P(u, \xi)$.

4.1 Scheme A

The first step in the derivation of the asymptotic behavior is to relate ξ to the initial density contrast. This can easily be done by substituting the expression (11) for L in (21), and using (18) and (25). The result is

$$\frac{\xi^2 - \xi^{\gamma+1}}{\xi^2 - 1} = -\alpha(\alpha - 1)(\gamma - 1)\delta_i^2. \quad (31)$$

Since $\delta_i \ll 1$ this relation implies that $\xi \ll 1$ as well. Retaining only the lowest order in ξ , the relation gives $\xi \propto \delta_i$ for $\gamma > 1$, and $\xi \propto \delta_i^{2/(\gamma+1)}$ for $\gamma < 1$. Since $r_a \leq r_*$, we have $r_b = \xi r_a \leq \xi r_* = \xi r_i \delta^{-1} < r_i$, i.e., the pericenter of a shell is smaller than its initial radius. Except near r_b , where a shell spends only a tiny fraction of its orbital time[†], the motion is almost radial. The initial radius, r_{ti} , of the shell currently at turnaround sets an upper limit on r_b . For $r \gg r_{ti}$ all shells move on almost purely radial orbits and the analysis of FG84 for collapse on purely radial motions apply. Therefore, according to FG84, we have

$$\gamma = p = \frac{3}{1 + 3\epsilon}, \quad s = q = 0, \quad \text{for } \epsilon \geq \frac{2}{3}, \quad (32)$$

and,

$$\gamma = 1, \quad q = \frac{3\epsilon - 2}{9\epsilon}, \quad s = 2q, \quad \text{for } \epsilon < \frac{2}{3}. \quad (33)$$

However r_{ti} tends to zero as $t_i \rightarrow 0$. So for cosmological initial conditions in which $t_i \rightarrow 0$ the the collapse is identical to that of particles on purely radial motions.

4.2 Scheme B

The angular momentum in this scheme is given by (13). So the relation (21) gives

$$\frac{\xi^2 - \xi^{\gamma+1}}{\xi^2 - 1} = -\mathcal{L}^2(\gamma - 1), \quad (34)$$

implying that ξ is the same for all particles. The radius $r_t \xi$ is an upper limit on the pericenters of all shells. So only particles which have passed their turnaround radii early enough can contribute to the density at $r \leq r_t \xi$. Particles at $r \ll r_t \xi^2$ have their apocenters inside $r_t \xi$ as well, and so the radius $r_t \xi^2$ marks the boundary of the inner region where we expect the same power law behavior for the mass distribution. In this region only particles with $r_b = \xi r_a \leq r$, i.e., $u \geq \xi$ contribute to the integral in (29), so

$$\left(\frac{r}{r_t} \right)^{\gamma-p} = \frac{1}{p} \int_{\xi}^{\infty} du u^{-(1+p)} P(u, \xi). \quad (35)$$

The integral is independent of r , therefore we must have $\gamma = p$ for all $\epsilon > 0$. Using the expression (30), and the relations (18) and (25), yields

$$\gamma = p = \frac{3}{1 + 3\epsilon}, \quad s = q = 0, \quad \text{for all } \epsilon > 0. \quad (36)$$

In the collapse with $L = 0$ (FG84) and in scheme A this result is correct only for $\epsilon \geq 2/3$.

If $\xi \ll 1$ then in the region $r_t \gg r \gg r_t \xi$ particles move on almost radial orbits and the analysis of FG84 for collapse with no angular momentum is applicable. Applying the analysis of FG84 in that region gives $\gamma = 1$ for $\epsilon \leq 2/3$ and $\gamma = p$, as in (36), for $\epsilon > 2/3$. Therefore, as r is increased, the mass profile index varies from $\gamma = p$ to

[†] Consider the orbit of a particle in the plane (r, ψ) where ψ is the angular position. The time spent near r_b can be estimated as $\Delta T = \int_{\psi_1}^{\psi_2} d\psi r^2/L < 2\pi r_m^2/L$, where r_m is a few times r_b . By (21) we find that $r_b^2/L \sim \xi^n T_c$ where $n > 0$ and T_c is the period of a circular orbit at the apocenter r_a . So the time fraction spent near r_b is negligible for $\xi \ll 1$.

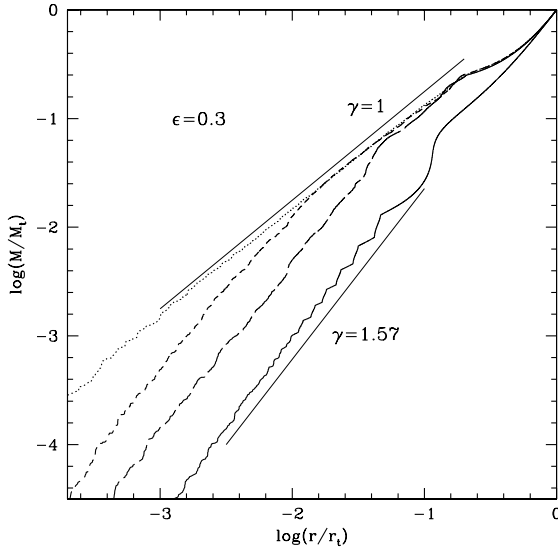


Figure 1. Mass profiles from spherical N-body simulations in which particles acquire angular momenta according to scheme B. The initial density perturbation has $\epsilon = 0.3$. The solid, long dashed, short dashed, and dotted curves are, respectively, mass profiles for $\mathcal{L} = 0.9, 0.3, 0.1, 0.001$.

$\gamma = 1$ for $\epsilon \leq 2/3$, but remains $\gamma = p$ for $\epsilon > 2/3$. In figure 1 we show the mass profiles obtained from spherical N-body simulations of 12000 shells for $\epsilon = 0.3$ with angular momentum introduced according to scheme B. The curves correspond, respectively, to simulations with $\mathcal{L} = 0.9$ (solid), 0.3 (long dashed), 0.1 (short dashed), and 0.001 (dotted). To save CPU, a shell participates in the simulation only after it reaches its turnaround radius. A fourth order Runge-Kutta time integration is used to integrate the equations of motion. The mass profiles in the figure behave as predicted from our analysis. A particle with $\mathcal{L} = 0.9$ moves in an almost circular, so that it effectively circles the halo at a radius slightly smaller than its turnaround radius. Therefore the corresponding mass profile (solid curve) would have an index close to $\gamma = 3/(1+3\epsilon) = 1.57$ almost for all $r < r_t$. The mass profile in the inner regions for $\mathcal{L} = 0.3$ and 0.1 (long and short dashed, respectively) have $\gamma \approx 1.57$, while in the outer regions it becomes ≈ 1 . For $\mathcal{L} = 0.001$, particles move on almost radial orbits over the whole distance range shown in the plot. Hence $\gamma \approx 1$.

5 DISCUSSION

We have studied the effect of non-radial motions on the mass profile of spherical self-similar collapse. Assigning angular momentum at the initial time does not affect the evolved mass profile. This is not surprising as the initial kinetic energy is dominated by the radial Hubble expansion velocity $\propto r/t_i$. Any additional finite velocity is negligible compared to the Hubble expansion velocity as $t_i \rightarrow 0$. This has also been shown explicitly for collapse with purely radial motions where a finite radial velocity component is superimposed on the Hubble expansion at the initial time (e.g., Peebles 1980, Padmanabhan 1993). We have also considered the conse-

quences of a different scheme (scheme B) for assigning angular momenta to particles. In scheme B, a particle acquires its angular momentum at maximum expansion. The acquired angular momentum is chosen in such a way that the ratio of the pericenter to apocenter is the same for all particles and no additional physical scale is introduced. In this case we have confirmed the conjecture by White & Zaritsky (1991) that the scaling $M \propto r^{3/(1+3\epsilon)}$ is maintained for all ϵ as $r \rightarrow 0$. But we have also shown that if the added angular momentum is small, then the behavior $M \propto r$ is restored far enough from the center for a perturbation with $\epsilon \leq 2/3$.

What is the justification for scheme B in a generic collapse configuration? Consider a halo forming in a gravitational collapse of a high density region in an initial scale free random Gaussian. The infalling matter is distributed in clumps (satellites). If the halo is approximately spherical then the collapse process cannot introduce any additional scale and angular momentum must be proportional to the product of the mass and the radius at the epoch of maximum expansion. But scheme B also assumes that the angular momentum of a particle is negligible before it reaches maximum expansion. This is a reasonable assumption if angular momentum is mainly generated by tidal interaction between the infalling satellites themselves. Because the halo is assumed spherical, the halo-satellite tidal interaction is not expected to generate any angular momentum with respect to the halo center. The assumptions underlying scheme B are consistent with results of N-body simulations (e.g., Barnes & Efstathiou 1987). Adiabatic invariance was also applied to non scale free initial density perturbations (Hoffman & Shaham 1985, Ryden & Gunn 1987, Lokas 2000, Lokas & Hoffman 2000). N-body results imply that in these situations as well, it is reasonable to introduce angular momentum according to scheme B.

6 ACKNOWLEDGMENT

The author thanks L. Chuzhoy and Y. Hoffman for stimulating conversations.

REFERENCES

- Avila-Reese V., Firmani C., Hernandez X., 1998, ApJ, 505, 37
- Bahcall N., Fan X., 1998, ApJ, 504, 1
- Bardeen J.M., Bond J.R., Kaiser N., Szalay A.S., 1986, ApJ, 304, 15
- Barnes J., Efstathiou G., 1987, ApJ, 319, 575
- Bartelmann M., Schneider P., 1999, astro-ph/9912508
- Bertschinger E., 1985, ApJS, 58, 39
- Chuzhoy L., Nusser A., 2000, astro-ph/0005331
- Fillmore J.A., Goldreich P., 1984, 281, 1
- Gunn J.E., 1977, ApJ, 218, 592
- Gurevich A.V., Zybin K.P., 1988a, ZHETF, 94, 3
- Gurevich A.V., Zybin K.P., 1988b, ZHETF, 94, 5
- Hoffman Y., Shaham J., 1985, ApJ, 297, 16
- Jing Y.P., 2000, ApJ, 535, 30
- Klypin A., Kravtsov A.V., Bullock J., Primack J., 2000, astro-ph/0006343
- Landau L.D., Lifshitz E.M., 1976, *Mechanics*, Pergamon Press
- J.E., 1986, ApJ, 318, 15
- Moore B., 1994, Nature, 370, 629
- Nusser A., Sheth R., 1999, MNRAS, 303, 685

Padmanabhan T., 1993, *Structure formation in the universe*, Cambridge University Press, Cambridge UK.

Peebles P.J.E., 1980, “*The Large Scale Structure in The Universe*”, Princeton University Press, Princeton.

Persic M., Salucci P., Stel F., 1996, MNRAS, 281, 27

Sarazin C.L., RvMP, 58, 1

Syer D., White S.D.M., 1998, MNRAS, 293, 227

Weinberg M., 2000, astro-ph/0007276

White S.D.M., Zartizky D., 1992, ApJ, 394, 1

Zaritsky D., White S.D.M., 1994, 1994, ApJ, 435, 599

Zaroubi S., Hoffman Y., 1992, ApJ, 416, 410